# Cloning and production of antisera to human placental 11 beta-hydroxysteroid dehydrogenase type 2

# Cloning and production of antisera to human placental 11$\beta$-hydroxysteroid dehydrogenase type 2

Roger W. BROWN*§, Karen E. CHAPMAN*, Yuri KOTELEVTSEV*‡, Joyce L. W. YAU*, Robbie S. LINDSAY*, Lawrence BRETT†, Caroline LECKIE*, Parvez MURAD*, Val LYONS*, John J. MULLINS‡, Christopher R. W. EDWARDS* and Jonathan R. SECKL*

University Departments of *Medicine and †Pathology, Western General Hospital, Edinburgh EH4 2XU, and ‡The Centre for Genome Research, Edinburgh, Scotland, U.K.

By inactivating potent glucocorticoid hormones (cortisol and corticosterone), 11$\beta$-hydroxysteroid dehydrogenase type 2 (11$\beta$-HSD2) plays an important role in the placenta by controlling fetal exposure to maternal glucocorticoids, and in aldosterone target tissues by controlling ligand access to co-localized glucocorticoid and mineralocorticoid receptors. Amino acid sequence from homogeneous human placental 11$\beta$-HSD2 was used to isolate a 1897 bp cDNA encoding this enzyme (predicted $M_r$ 44126; predicted pI 9.9). Transfection into mammalian (CHO) cells produces 11$\beta$-HSD2 activity which is $NAD^+$-dependent, is without reductase activity, avidly metabolizes glucocorticoids ($K_m$ values for corticosterone, cortisol and dexamethasone of $12.4 \pm 1.5$, $43.9 \pm 8.5$ and $119 \pm 15$ nM respectively) and is inhibited by glycyrrhetinic acid and carbenoxolone ($IC_{50}$ values 10–20 nM). Rabbit antisera recognizing 11$\beta$-HSD2 have been raised to an 11$\beta$-HSD2-(370–383)-peptide–carrier conjugate. Recombinant 11$\beta$-HSD2, like native human placental 11$\beta$-HSD2, is detectable with affinity labelling and anti-11$\beta$-HSD2 antisera, and appears to require little post-translational processing for activity. 11$\beta$-HSD2 mRNA ($\sim$ 1.9 kb transcript) is expressed in placenta, aldosterone target tissues (kidney, parotid, colon and skin) and pancreas. *In situ* hybridization and immunohistochemistry localize abundant 11$\beta$-HSD2 expression to the distal nephron in human adult kidney and to the trophoblast in the placenta. 11$\beta$-HSD2 transcripts are expressed in fetal kidney (but not lung, liver or brain) at 21–26 weeks, suggesting that an 11$\beta$-HSD2 distribution resembling that in the adult is established by this stage in human development.

## INTRODUCTION

Placental 11$\beta$-hydroxysteroid dehydrogenase (11$\beta$-HSD) metabolizes the potent glucocorticoids cortisol and corticosterone to inert 11-dehydro products (cortisone and 11-dehydrocorticosterone respectively) and thus protects the fetus from the deleterious effects of the higher glucocorticoid levels in the maternal circulation [1,2]. This protective placental enzyme barrier is very efficient so that almost all maternal cortisol is inactivated [3], ensuring that in late gestation the majority of cortisol reaching fetal tissues is derived from the fetal adrenals [4]. A relative deficiency of this enzyme in both rats and humans correlates with low birth weight [5,6]. Moreover, administration of the 11$\beta$-HSD inhibitor carbenoxolone to pregnant rats results in offspring with reduced birth weight and hypertension in adulthood (R. S. Lindsay, R. M. Lindsay, C. R. W. Edwards and J. R. Seckl, unpublished work). These effects parallel the well documented human epidemiological association between low birth weight and hypertension in adult life [7].

The 11$\beta$-HSD activity in placenta (11$\beta$-HSD2) is due to an isoform distinct from the previously characterized bi-directional NADP(H)-dependent enzyme (11$\beta$-HSD1) originally purified from liver [8]. Thus placental 11$\beta$-HSD2 has a higher affinity for glucocorticoid, is $NAD^+$-dependent and acts as an exclusive 11$\beta$-dehydrogenase (always inactivating glucocorticoids) [9]. Closely related or identical 11$\beta$-HSD2 enzyme activities have been described in rabbit renal cortical collecting duct cells [10], renal tissue from other species [11], and several human fetal tissues [12]. This enzyme activity in the distal nephron excludes glucocorticoids from otherwise non-selective mineralocorticoid receptors, so producing aldosterone selectivity in the face of a 1000-fold molar excess of circulating cortisol [13,14]. In the accompanying paper [15] we report the purification to homogeneity of human placental 11$\beta$-HSD2. Here we describe the isolation of a cDNA clone encoding human placental 11$\beta$-HSD2, the tissue distribution of the corresponding mRNA and studies examining the characteristics of the expressed protein and enzyme activity. In addition, we have raised antisera allowing the detailed localization of the 11$\beta$-HSD2 protein.

## EXPERIMENTAL

### Materials

$^3H$-, $^{35}S$- and $^{32}P$-labelled compounds, Hybond N and Hybond enhanced chemiluminescence (ECL) membranes, Hyperfilm $B_{max.}$, Sequenase v2 and the ECL Western blotting systems were purchased from Amersham International (Little Chalfont, Bucks., U.K.). *Asc*I was obtained from New England Biolabs (Hitchin, U.K.). PGEM-11zf($\pm$) plasmids, micrococcal nuclease-treated canine pancreatic microsomes (cat. no. Y4041) and other restriction enzymes were obtained from Promega (Southampton, U.K.). Synthetic oligonucleotides were synthesized by Oswel DNA Service (Edinburgh, Scotland, U.K.). DNA size markers (1 kb ladder), Lipofectin, media and reagents for tissue culture were purchased from Gibco–BRL (Paisley, Scotland, U.K.).

Abbreviations used: 11$\beta$-HSD(2), 11$\beta$-hydroxysteroid dehydrogenase (type 2); SAME, syndrome of apparent mineralocorticoid excess; ECL, enhanced chemiluminescence; RT-PCR, reverse transcription-PCR; UTR, untranslated region; TBS, Tris-buffered saline; DHEA(S), dehydroepiandrosterone sulphate; SCAD, short-chain alcohol dehydrogenase.

§ To whom correspondence should be addressed.

The nucleotide sequence data reported have been submitted to the Genbank/EMBL/DDBJ Nucleotide Sequence Databases under accession no. U26726.

Vectastain *Elite* ABC and DAB reagent system for immunohistochemistry was purchased from Vector Laboratories (Peterborough, U.K.). Reagents and molecular biology grade chemicals were purchased from Sigma Chemical Co. (Poole, Dorset, U.K.).

### Degenerate primer PCR and cloning of 11$\beta$-HSD2 fragment

Tissue was snap-frozen and RNA was extracted as described [16]. RNA was treated with DNase I, re-extracted to remove any contaminating genomic DNA and reverse transcribed using the Promega Reverse Transcription system (cat. no. A3500) according to the manufacturer's instructions. Inosine-containing degenerate primers were designed based on the amino acid sequence of five 11$\beta$-HSD2 tryptic peptides: A, B, B2, C and D (t = top strand, b = bottom strand) [15]. The primers from peptides B and C generated the most useful results and had the following sequences (where I is inosine): Bt, 5′-CA(A/G)GA(C/T)GCIGCICA(A/G)GA(T/C)CCIAA-3′; Bb, 5′-A(A/G)(A/G)TTIGG(A/G)TC(C/T)TGIGCIGC(A/G)TC-3′; Ct, 5′-(A/T)(C/G)ICCIGCIGGI(A/G)(A/C)IATGCCITA-3′; Cb, 5′-AGCICCIA(A/G)IIIIGG(A/G)TAIGGCAT-3′. Initial screening used the following protocol. A 5 $\mu$l sample of human placental cDNA was heated, under mineral oil, at 96 °C for 10 min and placed on ice. The reaction mixture was then added in a volume of 45 $\mu$l to give a final reaction mix containing 70 pmol of each degenerate primer, 50 $\mu$mol of dNTP and 2 units of Taq polymerase in 1 × PCR buffer (Promega, Southampton, U.K.). Reactions were placed into a thermal cycler (HB-TR1; Hybaid, Teddington, U.K.) with the block held at 90 °C and the programme commenced: 5 cycles of 60 s at 95 °C, 45 s at 43 °C, 43 → 55 °C at 1 °C/3 s and 90 s at 72 °C, followed by 35 cycles of 60 s at 95 °C, 60 s at 50 °C and 90 s at 72 °C, and finally 10 min at 72 °C. Subsequently a specific DNA product (of 531 bp) was efficiently amplified using the Ct/Bb primer pair and the following programme: five cycles of 60 s at 95 °C, 60 s at 47 °C, 47 → 50 °C at 1 °C/5 s, 50 → 55 °C at 1 °C/2 s and 150 s at 72 °C, followed by 40 cycles of 60 s at 95 °C, 60 s at 50 °C, 50 → 55 °C at 1 °C/s and 150 s at 72 °C, and finally 10 min at 72 °C. This allowed the 531 bp product to be directly cloned into pCRII (TA Cloning system v2; Invitrogen, San Diego, CA, U.S.A.: cat. no. K2000-01) to yield clone pCRIICtBb.

### PCR screening of a pcDNA1 human placental cDNA library

Specific PCR primers nested within this 531 bp fragment were designed [top primer (SCt), 5′-ATCCGTGCTTGGGGGCCTA-TGGAACCT-3′; bottom primer (SBb), 5′-CTGCAGTGCTCG-AGGCAGACAGTGACT-3′]. These produced a strong band of the expected size (455 bp) as the only product amplified by reverse transcription (RT)-PCR of human placental RNA. A human placental cDNA library in pcDNA1 (Invitrogen; A900-11) was then screened by increasing dilutions using this 455 bp product to detect positive pools and adapting the PCR screening method of [17] for use with plasmid libraries. Other specific primers were used to cross-check positives. PCR with one primer to the pcDNA1 vector arm and the other to the insert was used to estimate clone insert size. A partial 11$\beta$-HSD2 clone was isolated. On re-screening only one clone (> 1.9 kb) long enough to be full length [with coding region (40000-$M_r$ protein) plus 3′ untranslated region (UTR) being ⩾ 1.7 kb] was found, but this produced no 11$\beta$-HSD activity on expression in CHO cells.

### Screening of a $\lambda$DR2 cDNA library

A $\lambda$DR2 human placental cDNA library (Clontech, Palo Alto, CA, U.S.A.; HL1144x), with a higher proportion of longer cDNA inserts, was screened by conventional means using the incomplete 11$\beta$-HSD2 sequence isolated from the pcDNA1 library. Briefly, 700000 plaques were plated and duplicate filter lifts were made, denatured, fixed, rinsed, dried and UV cross-linked before hybridization in SSC/formamide buffer (6 × SSC, 50 % formamide, 5 × Denhardt's solution, 0.5 % SDS, 100 $\mu$g/ml salmon sperm DNA) with random primed [$^{32}$P]dCTP-labelled probe from the incomplete 11$\beta$-HSD2 sequence. Washes were SSC/SDS-based, finishing with one 15 min wash at 65 °C in 0.2 × SSC/0.1 %SDS. Positives from the primary screen were purified by a secondary screen at low density. Secondary positives were converted from phage ($\lambda$DR2) to plasmid (pDR2) clones by means of the endogenous CRE/LOX recombinase of the host bacterial strain (*Escherichia coli* AM1) [18] and were tested for 11$\beta$-HSD2 enzyme activity by transfection into CHO cells, as described below. Nucleotide sequences were determined following sequencing of both strands by the dideoxy termination method using Sequenase v2 (Amersham/USB).

### Nucleic acid and protein sequence analysis

The 11$\beta$-HSD2 cDNA sequence and predicted 11$\beta$-HSD2 protein sequence were analysed using the computing facilities at the HGMP Resource Centre (Cambridge, U.K.) [19], specifically PredictProtein [20] and the GCG package [21]. Protein secondary structure was predicted by three methods, according to (1) Chou–Fasman as amended for overall structure probability [22,23], (2) Garnier–Osguthorpe–Robson [24], (3) and Rost–Sander [20]. The features described are for regions where there was no disagreement in predictions, while Figure 2 (middle panel) also extends illustration to areas (grey regions) with complete concordance between two predictions and where the third 'dissenting' prediction is not in complete agreement. Assessment of hydrophobicity was based on the Kyte–Doolittle index [25], while prediction of flexible and exposed/buried regions was according to the methods of Karplus–Schulz [26] and Emini et al. [27] respectively. Estimates of percentage identity in nucleic acid and protein alignments used the GAP algorithm [21] with standard settings of gap weight = 3 and length weight = 0.1 for protein alignment.

### *In vitro* translation

The 11$\beta$-HSD2 cDNA was subcloned into pGEM-11zf oriented so that the 5′ end of the cDNA was adjacent to the vector T7 promoter. *In vitro* translation was performed with a T7 polymerase driven, rabbit reticulocyte-based, coupled transcription/translation system (TNT lysates; Promega; L4610), to which a methionine-deficient amino acid mixture and [$^{35}$S]methionine were added. In a standard volume of 25 $\mu$l, 0.5 $\mu$g of subcloned 11$\beta$-HSD2 plasmid DNA was added. Microsomal co-translational processing was examined by including 0–4.5 $\mu$l of micrococcal nuclease-treated canine pancreatic microsomes in the standard 25 $\mu$l incubation at 30 °C for 90 min. Control reactions to verify signal peptide cleavage (0.1 $\mu$g of *E. coli* $\beta$-lactamase mRNA) and glycosylation (0.1 $\mu$g of *Saccharomyces cerevisiae* $\alpha$-factor mRNA) activities of the microsomes were carried out in parallel. For autoradiography, 0.05–5 $\mu$l of each reaction was run per lane on SDS/PAGE, stained with Coomassie Blue, processed in Entensify fluoroautoradiography solutions (NEN/DuPont, Stevenage, U.K.), dried and exposed to Kodak X-OMAT AR film.

### CHO cell transfection

CHO cells were maintained in Dulbecco's modified Eagle's

medium supplemented with 15% fetal calf serum, 100 units/ml penicillin, 100 $\mu$g/ml streptomycin and 200 mM glutamine. At 24 h prior to transfection cells were seeded on to dishes at a density of $2 \times 10^6$ cells/100 mm plate. For transfection, 5 $\mu$g of DNA (in 800 $\mu$l of Optimem) was mixed with 42 $\mu$l of Lipofectin (in 800 $\mu$l of Optimem) and incubated for 15 min at room temperature. Optimem was added to 10 ml and the mixture was gently overlaid on to cells which had been washed in Optimem. After 24 h the Optimem/DNA mix was removed and replaced with normal medium. Cells were harvested 24 h later. The human placental 11$\beta$-HSD2 cDNA was transfected into cells using the clone (in pDR2) isolated from library screening and there were appropriate controls for transfection efficiency. Assays of 11$\beta$-HSD activity were either with intact cells ([$^3$H]steroid added to the medium within the last 24 h, as described [28]) or using homogenates of scraped cells (as below).

### Kinetic and inhibitor studies

CHO cells were scraped, homogenized [$2 \times 10^6$ cells/0.5 ml of Buffer C (0.02 M Tris, pH 7.7, 10% glycerol, 1 mM EDTA, 300 mM NaCl)], centrifuged briefly (15000 ***g***, 15 s to pellet heavy debris, and the supernatant assayed for protein concentration and 11$\beta$-HSD2 activity essentially as described [15]. 11$\beta$-HSD2 assays contained 400 $\mu$M $NAD^+$, unless otherwise stated, and were analysed by HPLC when the [$^3$H]steroid concentration was $> 2.5$ nM; TLC-based analysis was also used at [$^3$H]steroid concentrations $< 5$ nM. Reaction products were identified (HPLC and TLC) by comparison with steroid standards run in parallel. Incubations were for 60 min (120 min for dexamethasone). Kinetic parameters were calculated from the initial-velocity determinations, obtained with experiments performed with a wide range of substrate concentrations (0.3, 0.4, 0.8, 1.5, 2, 3, 4, 8, 15, 20, 40, 80 and 150 nM [$^3$H]steroid, with 80 and 150 nM omitted for corticosterone). Enzyme concentrations giving less than 30% conversion were used. Control ('vector-only' transfected cells) and blank assays were carried out in parallel.

### 11$\beta$-HSD2 photoaffinity labelling

This was carried out as described in the accompanying paper [15], with the labelling performed at 0 °C. Transfected cells were homogenized, briefly centrifuged (1000 rev./min × 15 s) to pellet lumpy debris, and the supernatant labelled at 0.25 mg of protein/ml. Labelling reactions of the placental 25000 ***g*** pellet (at $\sim 0.15$ mg of protein/ml) were run in parallel. The post-labelling samples were acetone-precipitated and analysed by electrophoresis (SDS/PAGE) and fluoroautoradiography.

### Northern hybridization

Adult human tissue samples were obtained at surgery, frozen within 10 min and stored at −80 °C. Most samples were normal tissue removed adjacent to a tumour on resection; this was the case for kidney (with adjacent adrenal), parotid, colon (splenic flexure), breast (with adjacent skin and dermis) and stomach (with distal oesophagus). Normal ovary (pre-menopausal) was obtained at hysterectomy. Pancreas was an unaffected area in a pancreatic tail resected for chronic pancreatitis. Liver was from a partial hepatectomy in a young woman to remove a hepatic cyst (benign). Placenta was from a normal delivery. Regions of a normal human brain obtained *post mortem* (36 h) were also dissected. RNA was extracted as described [16], separated on denaturing agarose/formaldehyde gels ($\sim 10$ $\mu$g/lane) and blotted on to Hybond N membrane (Amersham). A human multiple tissue Northern blot was purchased from Clontech (7756-1). Highly purified poly(A) RNA (2 $\mu$g) from fetal tissues [brain, lung, liver (female) and kidney] recovered following spontaneous abortions (at least two specimens pooled for each organ) were run in each lane and blotted. The exact age ranges were: fetal brain, 21–26 weeks; fetal lung, 22–23 weeks; fetal liver, 22–26 weeks; fetal kidney, 19–23 weeks. Blots were hybridized with a randomly primed $^{32}$P-labelled p11$\beta$2 *Asc*I–*Dra*I fragment (bases 217–1737; see Figure 2) at 55 °C overnight in hybridization buffer (0.2 M sodium dihydrogen phosphate, 0.6 M disodium hydrogen phosphate, 5 mM EDTA, 6% SDS and 100 $\mu$g/ml denatured herring testis DNA). Washes were SDS/SSC-based, finishing with 0.1 × SSC/0.1% SDS at 65 °C followed by autoradiography (−70 °C; 3–8 days).

### *In situ* hybridization

Cryostat sections (10 $\mu$m) were cut from frozen samples of human kidney (normal tissue from the opposite pole to a discrete renal cell carcinoma) obtained at surgery and normal placenta. Sections were mounted on to gelatin- and poly(L-lysine)-coated slides, and stored at −80 °C. Slides were post-fixed in 4% paraformaldehyde, washed in 2 × SSC and incubated with pre-hybridization buffer for 3 h at 50 °C, as previously described [29], before hybridization with SP6-transcribed [$^{35}$S]UTP-labelled anti-sense cRNA probes from *Xba*I-linearized pCRIICtBb (531 bp of p11$\beta$2; bases 654–1184; dashed box in Figure 2, top panel). Sense controls used T7-transcribed cRNA primed from *Hin*dIII-linearized pCRIICtBb. RNA probes were denatured, added at a final concentration of $10 \times 10^6$ c.p.m./ml in hybridization buffer, applied to slides as described [29] and incubated overnight at 50 °C. Following hybridization, sections were rinsed twice in 2 × SSC, treated with RNase A (30 $\mu$g/ml, 60 min, 37 °C), and washed to a maximum stringency of 0.1 × SSC at 60 °C for 60 min. After dehydration in increasing concentrations of ethanol, slides were exposed to autoradiographic film (Hyperfilm $B_{max.}$). Slides were dipped in photographic emulsion (NTB-2; Kodak) and exposed in a light-tight box (D19; Ilford) for 5 weeks, before being developed and counterstained with 1% pyronin.

### Raising of antisera and immunohistochemistry

Solid-phase synthesis of an 11$\beta$-HSD2 peptide HCLPRALQPGQPGT (residues 370–383; see Figure 2) with high predicted antigenicity was carried out. The peptide was N-terminally coupled to keyhole limpet haemocyanin and rabbits were inoculated with the conjugate in Freund's adjuvant, boosting monthly. Antisera highly specific for 11$\beta$-HSD2 and reacting to the peptide were obtained after the fourth boost. Western blots were performed with the 11$\beta$-HSD2 antisera, at 1:10000 dilution (as primary antibody), using the Amersham ECL system and methods recommended by the manufacturer.

### Immunohistochemistry including pre-absorption with excess 11$\beta$-HSD2-(370–383)-peptide antigen

Sections of human tissue, stored at −80 °C, were thawed into neutral formalin fixative (for 8 h), paraffin-processed and 4 $\mu$m sections cut. After drying, sections were dewaxed, hydrated and treated in 3% $H_2O_2$ (20 min) and blocked with 20% sheep serum in TBS (Tris-buffered saline, pH 7.6, with 1% BSA and 0.1% sodium azide). This diluent was also used for primary and secondary antibodies. Immunostaining, using an avidin–biotin

complex (ABC) method at room temperature, was as follows: primary antibody (1:2000), 30 min; TBS wash; secondary antibody [1:400 biotinylated sheep anti-rabbit $F(Ab)_2$ fragments; Boehringer Mannheim, Lewes, W. Sussex, U.K.], 30 min; TBS wash; Vectastain ABC *Elite* reagent, 30 min; diaminobenzidine substrate/chromagen reagent, 5 min. Sections were counterstained in Mayer's haematoxylin, dehydrated, cleared and mounted. Primary antibody preparations used were (a) 11$\beta$-HSD2 antisera, (b) preimmune serum from the same rabbit and (c) 11$\beta$-HSD2 antisera pre-absorbed for 16 h with 11$\beta$-HSD2-(370–383)-peptide at 50 $\mu$g per ml of diluted antibody. Both (b) and (c) were used as controls for (a).

## RESULTS AND DISCUSSION

### Cloning of 11$\beta$-HSD2 from human placenta

Degenerate primers (based on five 11$\beta$-HSD2 tryptic peptide sequences, both strands) were used in all pairwise combinations in an initial RT-PCR screen carried out on human placental mRNA. Combinations involving primer Bb resulted in the amplification of several particularly prominent DNA products, the majority of which appeared to be independent of the top primer used (Figure 1, lanes 1–4), and indeed PCR with Bb alone reproduced many of these bands. A clear exception was the PCR product arrowed in Figure 1 (lane 2); this was specific to the CtBb primer pair and became the major product (Figure 1, lane 5) using more stringent PCR conditions. This CtBb fragment was directly cloned and sequenced, revealing a single open reading frame spanning its length (531 bp) and with a predicted amino acid sequence encompassing four 11$\beta$-HSD2 peptides (C, B, A and B3), including a short-chain alcohol dehydrogenase (SCAD) motif (YXXXK; see below). This CtBb fragment was used (a) to design a synthetic peptide to raise antisera (see below) and (b) to isolate a complete 11$\beta$-HSD2 cDNA.

A human placental cDNA library in pcDNA1 was initially screened by a PCR-based approach and a 1177 bp partial clone

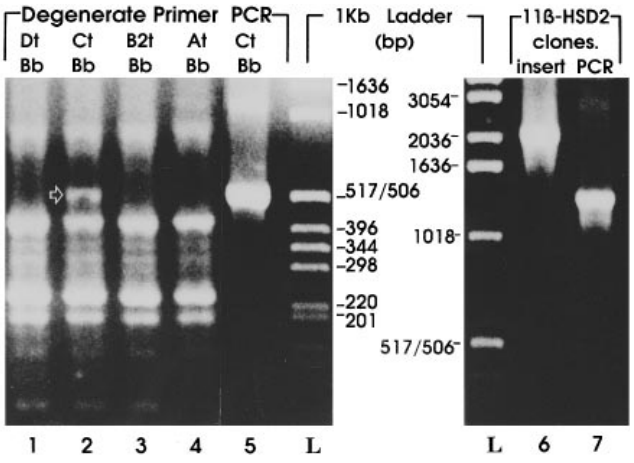


**Figure 1 PCR to amplify 11$\beta$-HSD2 sequences**

Ethidium bromide-stained agarose gels showing analysis of PCR amplifications. Lanes 1–5, RT-PCR on human placental mRNA using degenerate primers based on 11$\beta$-HSD2 peptide sequences A–D. Primers used (Xt = top; Xb = bottom; X = peptide) are indicated above the corresponding lane. Lanes 1–4, initial PCR conditions used; lane 5, more stringent amplification used, yielding only the CtBb specific product (531 bp) identified initially (arrowed, lane 2). Lanes 6 and 7, PCR (using vector-specific primers flanking the cloning sites) of 11$\beta$-HSD2 inserts of a 1179 bp partial pcDNA1 library clone [1157 bp + 22 bp poly(A); lane 7] and the 1919 bp [1897 bp + 22 bp poly(A)] pDR2 clone containing the full coding region (lane 6). Lanes L, 1 kb ladder (Gibco–BRL.)

isolated (Figure 1, lane 7) which contained the CtBb fragment, 45 bp further 5′ and 603 bp further 3′ [reaching to the 3′ end of the cDNA with a 22 bp poly(A) tail]. Conventional screening of 700000 plaques from a human placental DR2 library (Clontech), using the incomplete 11$\beta$-HSD2 sequence as a probe, allowed isolation of a single clone which, when converted to a pDR2 plasmid form (see the Experimental section), produced very abundant, $NAD^+$-dependent, 11$\beta$-HSD2 activity in transfected CHO cells. This clone was designated p11$\beta$2.

### Characteristics of the cDNA clone and predicted 11$\beta$-HSD2 protein sequence

#### General features of the 11$\beta$-HSD2 cDNA clone

This active 11$\beta$-HSD2 clone, p11$\beta$2, contained a 1897 bp cDNA with 22 bp poly(A) tail (1919 bp total), and has a G+C-rich composition (63.25%). The 5′ end of the cDNA (first $\sim$385 bases) is extremely G+C-rich (79.2%) and contains a 'CpG island' [30] with 56 occurrences (in 385 bases) of this usually scarce dinucleotide. The G+C and CpG content falls abruptly beyond this region (to 55% G+C; CpG frequency falls 4-fold). These features, which extend to the start of the 11$\beta$-HSD2 cDNA, are suggestive of a 5′ transcription regulatory region. The best candidate for initiation of translation is the ATG codon beginning 134 bases from the 5′ end of the cDNA (set to +1 in Figure 2, top panel); this is in a good context for initiation of translation, with 9/10 matches to the putative ideal ribosome binding site (GCCGCCATGG) [31], and is within the longest open reading frame ($-63 \rightarrow +1215$; Figure 2), defining a predicted coding region of 1215 bp ($+1 \rightarrow +1215$), flanked by a 5′ UTR of 133 bp ($-133 \rightarrow -1$) and a long 3′ UTR of 549 bp ($+1216 \rightarrow +1764$). The predicted coding region encodes a 405-amino-acid protein (calculated $M_r$ 44126) encompassing all the 11$\beta$-HSD2 peptide sequence derived from digests of the purified protein [15] (boxed in Figure 2). The most abundant amino acids are leucine (68 residues in 11$\beta$-HSD2), alanine (46) and glycine (32), which are all highly represented in proteins in general, followed by proline (32) and arginine (30). The high arginine content seems responsible for the very basic nature of the 11$\beta$-HSD2 protein, so clear during purification, as basic residues (Arg = 30, Lys = 12, His = 7) markedly outnumber acidic ones (Asp = 15, Glu = 15), giving a predicted net positive charge (+19) and a very basic predicted isoelectric point of 9.92 for the 11$\beta$-HSD2 polypeptide. Nine cysteine residues are present, one of which occupies the position at which a blank cycle resulted on sequencing of an 11$\beta$-HSD2 peptide (cycle 15, peptide C) [15], suggesting that this residue may be particularly reactive or modified in the native protein.

#### Detailed analysis of the predicted structure of the 11$\beta$-HSD2 protein

Analysis of the primary structure (Figure 2, top panel) and the predicted secondary structure (Figure 2, middle panel) of the 11$\beta$-HSD2 protein suggests four distinct regions. The most N-terminal region (region I) begins with an exposed loop (Met-1–Gly-9) followed by a very leucine/alanine-rich area (60% of residues 11–73). This has some incomplete repeats (AALALLAAL; residues 36–44; close variants beginning at residues 16 and 56) and appears likely to have secondary structure broken by helix-breaking residues (Gly-31 and Pro-33; Pro-53–Pro-54–Pro-55) into three buried, predicted $\alpha$-helical, segments centring on residues 16–22, 35–41 and 63–69 respectively. The region has imperfect heptad symmetry, and in such a secondary structure is likely to form a particularly hydrophobic

face along which leucines align, there being two such potential axes: (1) L14-L21-L28-L35-A42, stretching around to the nearby helical face L13-L20-D27-L34-L41, and (2) reaching further C-terminal in the region L23-L30-A37-L44-L51-L58-G65-L72. On the helical aspect opposite to these axes all seven positively charged residues in the area line-up: R18-R25-R32–-R74 and R29–R50–R71. Such a structure is suggestive of a domain with a leucine-zipper-like tendency to form protein–protein interactions (often dimerization) along the hydrophobic axes.

The second region (region II), which unlike the rest of the protein has predicted secondary structure rich in β-sheets, contains three motifs characteristic of members of the SCAD superfamily. Firstly, the putative cofactor-binding site motif (V/I)TGXXXGXG is present (ITGCDSGFG; residues 87–95) in an area with secondary structure predicted to incorporate buried β-sheet (residues 84–88), buried loop (89–92) and an exposed helix (96–102). Secondly a 'substrate positioning' motif, noted in previous alignments of SCAD enzymes [32], which is of the form [LFVM][VI][NL][N][AVH(F)][GI], is present (LVNNAG; residues 164–169). The major predicted features of this substrate positioning area are an exposed loop (residues 156–160)/buried β-sheet (161–166+) being preceded by an α-helix (centred on residues 145–152) and exposed flexible region likely to loop around Pro-142–Gly-143. Thirdly, the putative catalytic motif YXXXKX(SAG) is present (YGTSKAA; residues 232–238). This motif, which is predicted to form a small loop around Gly-233, is in the centre of a stretch predicted to have flanking areas consisting of loop → buried β-sheet → loop structures (at 211–223 and 252–264). A long hydrophobic α-helix (residues 236–250) bridges the motif-loop/sheet/loop stretch to the C-terminal side; however, the secondary structure is unclear for the region (residues 224–231) bridging between the motif and the loop/sheet/loop on the N-terminal side. The equivalent of this 'upstream bridging region' in the related SCAD enzyme 3α,20β-HSD was shown to be part of the steroid substrate (cortisone) binding pocket in X-ray crystallographic studies [33].

Region III (residues 275–370) has three positively charged segments, EKRKQ, ARPRRRY and LRRRF (residues 277–281, 332–338 and 358–362 respectively). Such segments may form charge interactions with negatively charged molecules or exert electrostatic influence on a substrate. In the context of a membrane protein, interactions with phospholipids helping to stabilize or anchor the protein are particularly likely and often occur adjacent to helical transmembrane domains (e.g. glycophorin [34]). Indeed most of the region between the charged segments has predicted helical secondary structure, especially residues 274–294, 298–312 and 324–331.

Finally region IV, the C-terminal region, is proline/glycine-rich (36% of residues 373–405) and is predicted to form a flexible area with several exposed loops. It contains the only potential N-glycosylation site in 11β-HSD2. The potential for glycosylation at this motif is weakened as it is flanked by prolines. Moreover, amino acid sequencing yields across the B peptide (Figure 2) suggested that Asn-394 was largely unglycosylated in the native protein from human placenta [15].

Although much of the secondary structure can be predicted with some certainty, there are important aspects of the higher-order structure of 11β-HSD2 that are unclear. As 11β-HSD2 is an intrinsic membrane protein from a family of enzymes (SCADs) thought usually to be tetrameric in the native form, it probably contains both transmembrane segments and dimerization interfaces. The N-terminal leucine/alanine-rich region (residues 11–73) may potentially fulfil either role, whereas the helical/charge cluster region (residues 275–370) contains predicted hydrophobic helical segments which are good candidates as possible transmembrane regions. Dimerizing elements outside the N-terminal region seem likely, as a number of other SCADs which lack such a region have been demonstrated to form tetramers. Figure 2 (middle panel) also illustrates the secondary structure of the related SCAD enzyme 3α,20β-HSD as determined from X-ray crystallography studies. There is a very striking similarity within region II (the SCAD region), with almost all the major structural features from βA–βF of 3α,20β-HSD being represented clearly in the predicted 11β-HSD2 structure [the only exception being that βB corresponds to a segment of 11β-HSD2 (residues 104–109) with uncertain secondary structure]. Studies on 3α,20β-HSD have identified areas involved in steroid and cofactor binding and in dimerization; some of the corresponding regions in 11β-HSD2 may have similar functions The dimerization interfaces of 3α,20β-HSD include the the region between the LVNNAG and YXXXK SCAD motifs (αE–βE–αF) and the most C-terminal β-sheet element (βG) [33].

### Sequence similarities to human placental 11β-HSD2

A search of sequence databases shows that the most clearly related proteins are SCAD members (Figure 2, bottom panel), the closest being microsomal $NAD^+$-dependent human 17β-HSD type 2 [35] (38.9% amino acid identity), retinal pigment epithelium $NAD^+$-dependent bovine 11-*cis*-retinol dehydrogenase (35.5% identity) and mitochondrial human $NAD^+$-dependent enzyme 3-hydroxybutyrate dehydrogenase [36] (32.6% identity). There is 28.3% identity to human 11β-HSD type 1 [37] (microsomal; $NADP^+$-dependent). Similarities of the four 11β-HSD2 regions (I–IV) are shown in Figure 2 for these enzymes and others with some functional similarity that are related to 11β-HSD2. The three SCAD motifs referred to above are highly conserved, although the middle motif is atypical in 11β-HSD1 and is shifted in relative position or absent in 3β-HSD2. This latter enzyme appears to have the other two SCAD motifs in the same orientation and with spacing typical of SCADs. This highlights the fact that members of the bifunctional 3β-HSD family (which share high sequence identity and also have ketosteroid isomerase activity) fit somewhat uncomfortably into the SCAD superfamily, and it is unclear whether they should be considered as SCADs or as a separate family. $NAD^+$-dependent 11β-HSD enzymes have been expression-cloned from kidney in sheep [38] and human [39]. The sheep kidney 11β-HSD2 has 78.5% identity at the protein level (82.6% at the nucleic acid level). Similarity is non-uniform across regions I–IV at both the protein (Figure 2) and nucleic acid levels; thus sheep 11β-HSD2 has 94.2%, 88%, 80% and 65% identity with human 11β-HSD2 at the cDNA level in regions I–IV respectively. The 5′ UTR and most of the 3′ UTR have ~70% identity; however, this rises sharply again between bases 1536 and 1624 (Figure 2, top panel) (91% identity; reason unclear) and for sequences adjacent to the polyadenylation motif aaataa (92%; bases 1731–1764; Figure 2). The human renal clone is similar, but not identical, to the cDNA from placenta reported here. The renal clone lacks the first 25 bases (−133 → −109), has two deletions in the 3′ UTR (bases 1270 and 1495; Figure 2) and a base substitution at 442 resulting in a change in the predicted amino acid sequence of Val-148 → Leu. At the points of difference, the sequence reported above has been confirmed in cDNA that we have sequenced derived from a second placenta, and the Val-148 residue is clearly present in human placental 11β-HSD2 as it is the first amino acid of the D peptide sequence derived from purified 11β-HSD2 tryptic digests. Although it is most likely that these differences arise from polymorphisms, there may be isoform

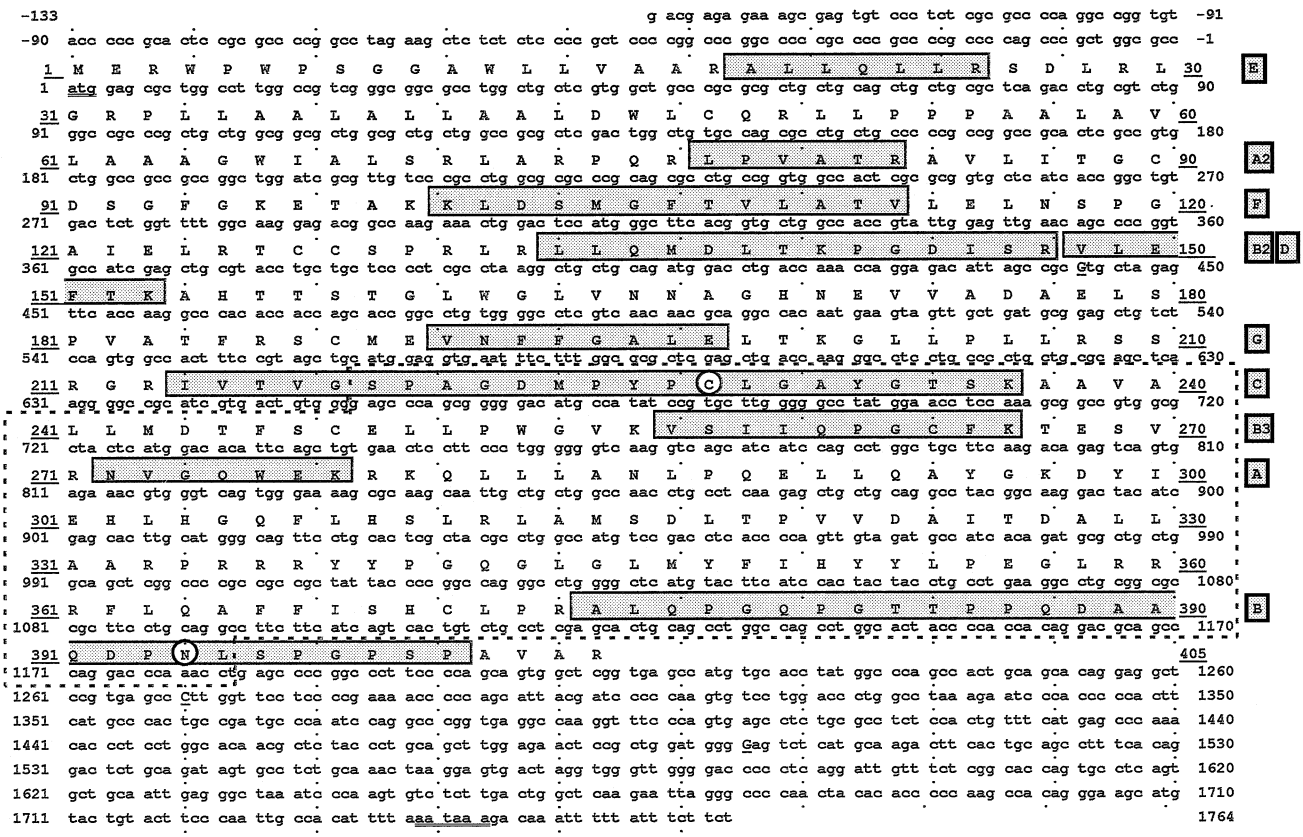

## Predicted Secondary Structure.

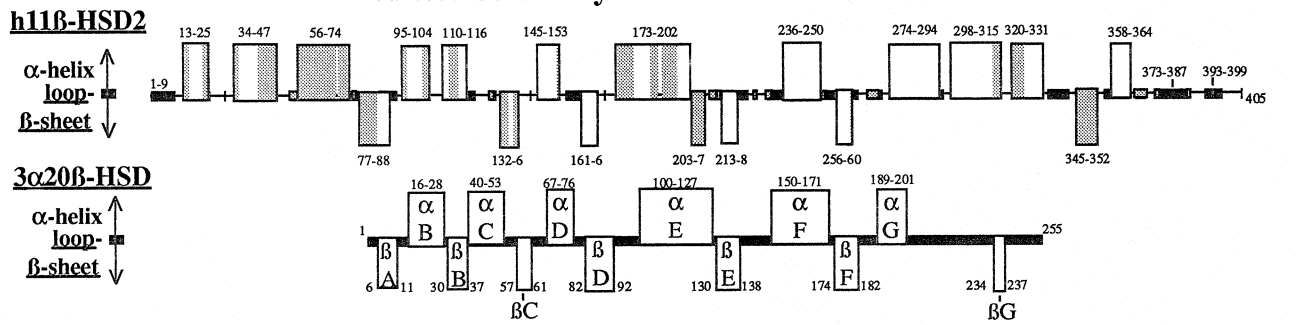


### Percent Amino Acid Identity

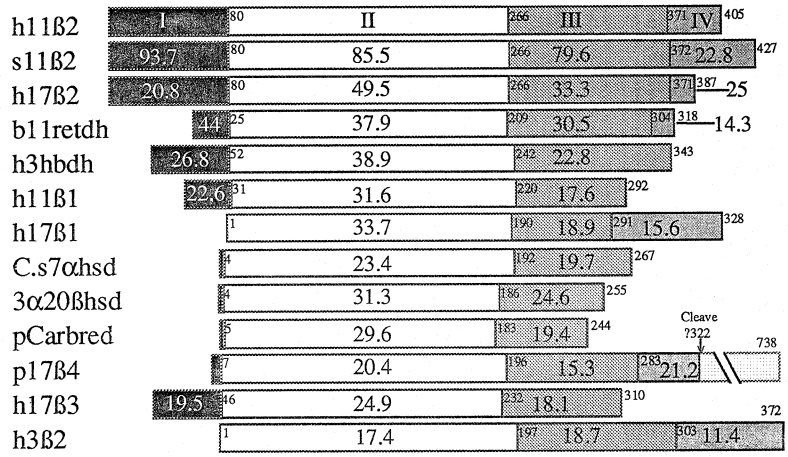


### Short Chain Alcohol Dehydrogenase Motifs

ITGCDSGFG-(X)$_{78}$-LVNNAG-(X)$_{69}$-YGTSKAA
ITGCDSGFG-(X)$_{78}$-LVNNAG-(X)$_{69}$-YGTSKAA
VTGGDCGLG-(X)$_{78}$-VINNAG-(X)$_{69}$-YGSSKAA
ITGCDSGFG-(X)$_{76}$-LVNNAG-(X)$_{68}$-YCVSKFG
VTGCDSGFG-(X)$_{82}$-LVNNAG-(X)$_{68}$-YCITKFG
VTGASKGIG-(X)$_{78}$-LILNHI-(X)$_{69}$-YSASKFA
ITGCSSGIG-(X)$_{78}$-LVCNAG-(X)$_{69}$-YCASKFA
VTSATRGIG-(X)$_{72}$-LVNNFG-(X)$_{67}$-YGVSKSG
ITGGARGLG-(X)$_{74}$-LVNNAG-(X)$_{69}$-YGASKWG
VTGAGKGIG-(X)$_{69}$-LVNNAA-(X)$_{70}$-YSSTKGA
VTGAGGGLG-(X)$_{83}$-VVNNAG-(X)$_{69}$-YSAAKLG
ITGAGDGIG-(X)$_{77}$-LVNNVG-(X)$_{71}$-YSASKAF
VTGAGGLLG-(X)$_{92}$-NVNVKG-(X)$_{57}$-YPYSKKL

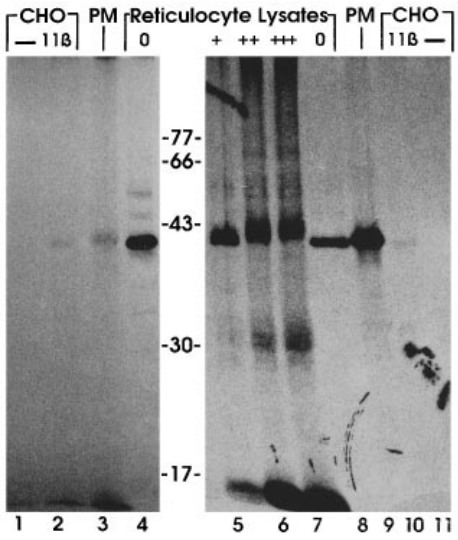


**Figure 3 Labelling of native, expressed and *in vitro* translated 11$\beta$-HSD2 protein**

Lanes 1–3 and 9–11: affinity labelling with [$^3$H]corticosterone of native human placental 11$\beta$-HSD2 from placental membrane fractions [PM; lanes 3 and 9; 20 and 80 $\mu$g of protein loaded respectively, from 25000 ***g*** pellet (heavy microsomal and mitochondrial fraction)] and from homogenates of CHO cells (160 mg of protein/lane) transfected with 11$\beta$-HSD2 cDNA (lanes 2 and 10) or with vector only (lanes 1 and 11). Lanes 4–8, products of coupled *in vitro* transcription/translation of 11$\beta$-HSD2 cDNA (subcloned into pGEM11zf) in rabbit reticulocyte lysates labelled with [$^{35}$S]methionine in the presence of various amounts of microsomes [indicated above lane: 0; + = 1.5 $\mu$l; ++ = 3 $\mu$l; +++ = 4.5 $\mu$l (excess)]. The lysate volume loaded in lanes 4–8 was 0.5, 1, 1, 1 and 0.1 $\mu$l respectively. The volume loaded was varied to facilitate size comparison of the translated products and was needed to counter the decrease in translation in the presence of higher microsome concentrations. The positions of protein standards ($10^{-3} \times M_r$) are indicated.

microheterogeneity similar to that observed with other steroid-metabolizing enzymes, notably 3$\alpha$-HSD (98.8 % identity) [40,41] and 3$\beta$-HSD (rat 3$\beta$-HSD2 being 99.2 % and > 93 % identical to 3$\beta$-HSD2 male liver variant [42] and 3$\beta$-HSD1 [43] respectively). The finding of polymorphisms that affect the 11$\beta$-HSD2 protein sequence is clearly of considerable interest, especially if they are associated with a difference in steroid metabolism. Placental 11$\beta$-HSD2 has a $K_m$ for corticosterone (see below; Table 1) virtually identical to that of the 1000-fold purified native 11$\beta$-HSD2 from placenta [9]. The $K_m$ reported for the renal clone is 3-fold lower (~ 4.4 nM), and it could be that amino acid substitutions at residue 148 cause subtle alterations in steroid-metabolizing activity by affecting the predicted $\alpha$-helical region of which it is part.

## Expression studies with human placental 11$\beta$-HSD2 cDNA

### Expression of 11$\beta$-HSD2 protein

Expression of p11$\beta$2 in CHO cells produced abundant 11$\beta$-HSD2 enzyme activity (see below), accompanied by the expression of an ~ 40000-$M_r$ protein which could be affinity-labelled with corticosterone (Figure 3, lanes 2 cf. 1 and 10 cf. 11), in a similar manner to the affinity labelling of 11$\beta$-HSD2 from crude placental subcellular fractions (Figure 3, lanes 3 and 9). Coupled *in vitro* transcription/translation of 11$\beta$-HSD2 in rabbit reticulocyte lysates (without microsomal processing) also produced a protein (Figure 3, lanes 4 and 8) of similar size to 11$\beta$-HSD2 in placenta or expressed in CHO cells. Thus activity in these tissues appears not to require major cleavages or large covalent attachments. Addition of canine pancreatic microsomes resulted in a small size increase and broadening of the protein band, suggesting that co-translational processing, possibly involving glycosylation, was occurring (Figure 3, lanes 4–8). Addition of increasing amounts of microsomes also resulted in a reduced efficiency of translation (a standard finding with TNT lysates); accordingly more sample was loaded (to facilitate size comparison), and a minor band at ~ 31000-$M_r$ became visible. It is unclear if this is a different, minor, translation product or the result of 11$\beta$-HSD2 proteolytic cleavage (processing or degradative) occurring at a low level in the presence of these microsomes. Clearly a range of processed states of 11$\beta$-HSD2 is demonstrated and may indicate the possibility of tissue-specific co-translational processing depending on the activities within host tissue microsomes. If cleavage to an ~ 31000-$M_r$ form occurs, this is likely to affect enzyme structure/function and possibly its subcellular localization. Finally, although native placental 11$\beta$-HSD2 is most likely to be located in microsomes, this is not confirmed by the presence of a classical C-terminal microsomal retention motif [44,45], in contrast to the closely related human 17$\beta$-HSD2 [35].

### Characteristics of expressed enzyme activity

Expression of the 11$\beta$-HSD2 cDNA in CHO cells produced high-affinity 11$\beta$-HSD activity which had the expected characteristics of 11$\beta$-HSD2 activity in placenta. This was exclusively $NAD^+$-dependent in cell homogenates (12 nM corticosterone and 0.15 mg of protein/ml), showing 49 % conversion with 400 $\mu$M $NAD^+$, whereas 400 $\mu$M $NADP^+$ produced no increase over assay with no added cofactor (1.8 %). No 11$\beta$-reductase activity was detected in homogenates of 11$\beta$-HSD2-transfected CHO cells, or in the medium of the intact cells (which metabolized 99 % of 25 nM [$^3$H]corticosterone in 24 h). 11-Dehydro products were the only metabolites detected by HPLC. Thus after a 1 h incubation of [$^3$H]steroid (12 nM) with recombinant 11$\beta$-HSD2

**Figure 2 cDNA and predicted amino acid sequence of human placental 11$\beta$-HSD2**

Top panel: the cDNA numbering (−133 to +1764; shown on the left of the DNA sequence) sets +1 at the start of the predicted coding region (note that the 'no base zero' convention is followed). The ATG initiation codon and polyadenylation motif are double-underlined. The broken line encloses the 531 bp CtBb fragment identified by RT-PCR (Figure 1, lane 5). Boxed sections of predicted amino acid sequence are those of the 10 peptides sequenced from tryptic digests of purified human placental 11$\beta$-HSD2; peptide nomenclature (small boxes) and numbering of the amino acid sequence are to the side of the sequence (amino acid sequence numbers are underlined). Circled residues are Cys-227 (unidentifiable residue on amino acid sequencing of peptide C) and Asn-394 (the only potential N-glycosylation site in 11$\beta$-HSD2, probably unused in placenta). Middle panel: predicted secondary structure of human placental 11$\beta$-HSD2 and that derived from X-ray crystallography for 3$\alpha$,20$\beta$-HSD from *Streptomyces hydrogenans* [33]. Segments represented as white ($\alpha$-helix, above line; $\beta$-sheet, below line) and black (loops; close to line) are of the greatest certainty; grey segments are of moderate certainty and segments represented by a flat line cannot be predicted with even moderate certainty. Bottom panel: alignment of 12 enzymes with sequence and functional similarity to human 11$\beta$-HSD2. On the left, percentage amino acid identity with regions I–IV of human 11$\beta$-HSD2 is indicated by larger-type numbers (small type indicates amino acid residue numbers at the start of regions). On the right, alignment of three motifs highly conserved in SCADs, with $(X)_n$ indicating that *n* amino acids separate the first residues of the adjacent motifs (inclusive). Enzymes are: h11$\beta$2 and s11$\beta$2, human and sheep 11$\beta$-HSD type 2 respectively; h17$\beta$1/2/3, human 17$\beta$-HSD types 1, 2 and 3; p17$\beta$4, pig 17$\beta$-HSD type 4; b11retdh, bovine 11-*cis*-retinol dehydrogenase; h3hbdh, human 3-hydroxybutyrate dehydrogenase; h11$\beta$1, human 11$\beta$-HSD type 1; C.s7$\alpha$hsd, 7$\alpha$-HSD from *Clostridium sordellii*; 3$\alpha$20$\beta$hsd, 3$\alpha$,20$\beta$-HSD from *Streptomyces hydrogenans*; pCarbred, pig carbonyl reductase; h3$\beta$2, human 3$\beta$-HSD type 2 (the adrenal/ovarian isoform).

**Table 1 Kinetic parameters of 11$\beta$-HSD2 activity in cells transfected with 11$\beta$-HSD2 cDNA**

All values are based on at least 10 steroid concentrations; $n = 5$ at each concentration for corticosterone and $n = 2$ for cortisol and dexamethasone. Aldosterone was not metabolized.

| Glucocorticoid | $K_m$ (nM) | $V_{max.}$ (pmol/h per mg of protein) |
|---|---|---|
| Corticosterone | 12.4 ± 1.5 | 8.0 ± 0.7 |
| Cortisol | 43.9 ± 8.5 | 4.8 ± 0.7 |
| Dexamethasone | 119 ± 15 | 3.7 ± 0.5 |
| Aldosterone | not metabolised | |

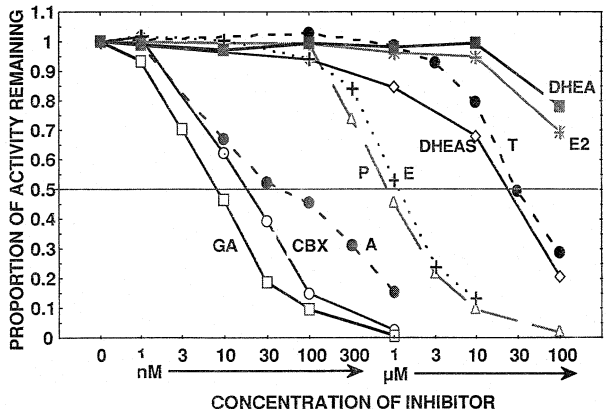


**Figure 4 Studies on inhibition of 11$\beta$-HSD2**

The extent to which a range of compounds inhibit the conversion of 12 nM [$^3$H]corticosterone by recombinant 11$\beta$-HSD2 is shown. GA, glycyrrhetinic acid; CBX, carbenoxolone; A, 11-dehydrocorticosterone; P, progesterone; E, cortisone; E2, oestradiol; DHEAS, DHEA sulphate. Reactions were in the presence of 400 $\mu$M $NAD^+$, using homogenates (0.15 mg of protein/ml) of cells transfected with 11$\beta$-HSD2 cDNA. Values are means of four determinations, with S.E.M.s $< 4\%$.

(0.5 mg of homogenate protein/ml), $> 95\%$ of corticosterone, 63% of cortisol and 17% of dexamethasone were metabolized, whereas aldosterone was unaltered. There was no evidence of 5$\alpha$- or 5$\beta$-reductase activity encoded by p11$\beta$2.

Recombinant human placental 11$\beta$-HSD2 has a high affinity for glucocorticoid substrates, especially corticosterone (Table 1). At corticosterone concentrations higher than 80 nM there appeared to be a degree of product/substrate inhibition. Examination of 11$\beta$-HSD2 inhibition ($IC_{50}$ values) by a range of steroids showed potent inhibition by glycyrrhetinic acid (11 nM) and carbenoxolone (18 nM), with significant inhibition by 11-dehydrocorticosterone (45 nM), progesterone (0.8 $\mu$M) and cortisone (1 $\mu$M), whereas there was little effect ($> 30$ $\mu$M) with dehydroepiandrosterone (DHEA), DHEA sulphate, testosterone and oestradiol (Figure 4). Affinity labelling studies (results not shown) on transfected CHO cells indicated the same rank order of potency in labelling [corticosterone $\gg$ cortisol $\gg$ dexamethasone (aldosterone = 0)] as indicated by their $K_m$ values (Table 1) as 11$\beta$-HSD2 substrates. A rank order of affinity as substrate/inhibitor is thus suggested for placental 11$\beta$-HSD2 of: glycyrrhetinic acid $\approx$ carbenoxolone $\approx$ corticosterone $>$ 11-dehydrocorticosterone $\approx$ cortisol $>$ dexamethasone $>$ progesterone $\approx$ cortisone $\gg$ DHEA sulphate $\approx$ testosterone $\approx$ oestradiol $\approx$ DHEA $\approx$ aldosterone. This rank order is very similar to that determined for the type III corticosterone receptor sites [46,47] and suggests that these sites are related to 11$\beta$-HSD2, but whether they are actually due to the 11$\beta$-HSD2 protein remains unclear. In late human gestation progesterone levels often rise to 0.3–0.5 $\mu$M in the mother and $> 1$ $\mu$M in the fetus [48]. Thus the $IC_{50}$ of progesterone for 11$\beta$-HSD2 (0.8 $\mu$M) may signify a potential influence of progesterone on corticosteroid action during late pregnancy.

## Distribution of 11$\beta$-HSD2 mRNA and protein in tissues

### 11$\beta$-HSD2 mRNA distribution

Northern analysis revealed a hybridizing $\sim 1.9$ kb transcript in the placenta, aldosterone target tissues (kidney, colon, parotid,

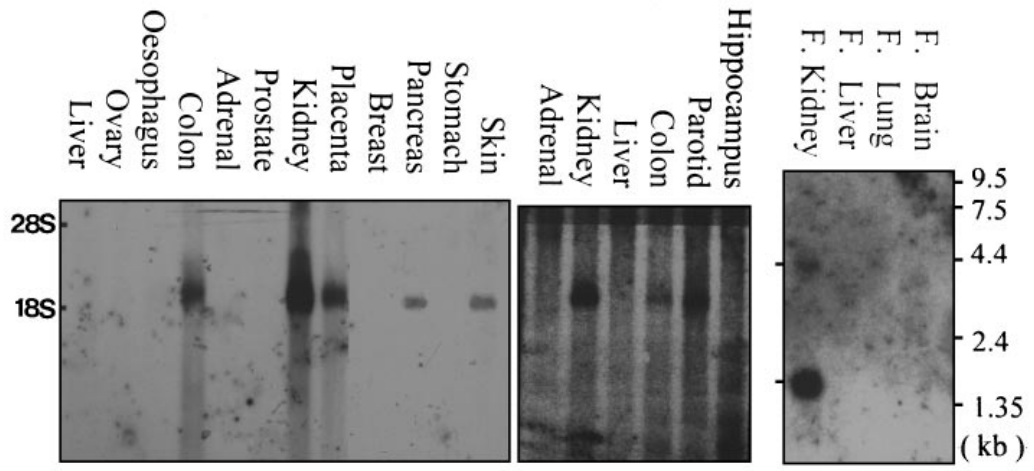


**Figure 5 Northern hybridization of 11$\beta$-HSD2 cDNA in human tissues**

Hybridization of RNA from a range of human adult (total RNA) and fetal [F.; highly purified poly(A) RNA] tissues with a random-primed human placental 11$\beta$-HSD2 cDNA probe (bases 217–1737; see Figure 2). Positions of fetal RNA markers and of 18 S and 28 S markers are indicated. Check-marks on left of the fetal-tissue blot correspond to the two mRNA species hybridizing, at $\sim$ 1.9 and $\sim$ 4 kb.

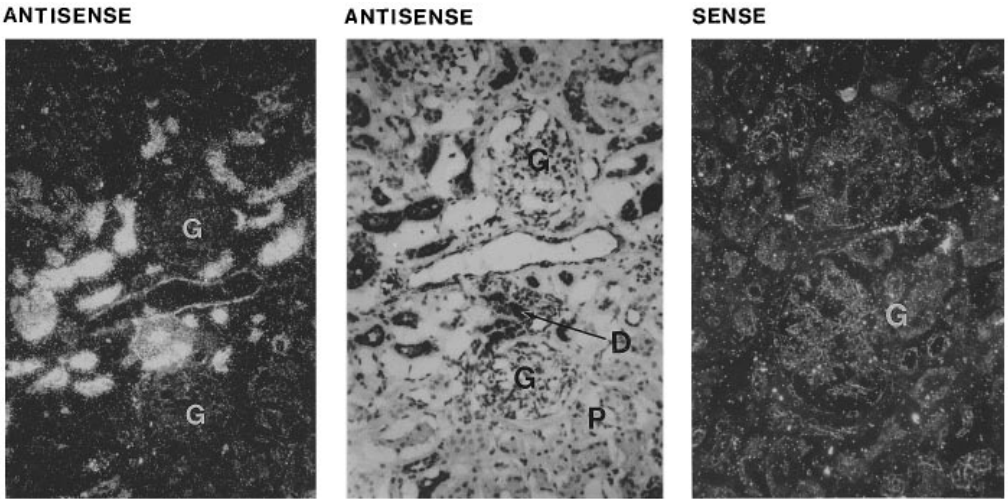


**Figure 6 11$\beta$-HSD2 *in situ* hybridization in human kidney**

*In situ* hybridization of sections of human kidney to human placental 11$\beta$-HSD2 cRNA probes (sense and antisense to CtBb fragment; dashed box in Figure 2). The middle panel shows a light field (silver grains = dark), whereas the other panels are dark field (silver grains = white). The left and middle panels are of the same section, the latter at a slightly higher magnification, whereas the right-hand panel is of a neighbouring section from the same kidney slice (at higher magnification). The following are labelled: G, glomerulus; D, distal convoluted tubule; P, area with many proximal convoluted tubules. Clearly 11$\beta$-HSD2 mRNA is abundant in the distal nephron.

skin), pancreas and fetal kidney (Figure 5). There was also hybridization to mRNA of a larger size ($\sim$ 4 kb) in fetal kidney. Under these conditions there was no detectable hybridization to RNA from liver, oesophagus, stomach, ovary, prostate, breast, fetal lung, fetal liver or fetal brain, or from adult human brain sub-regions (frontal cortex, cerebellum, hippocampus, hypothalamus, pons and medulla; results not shown). *In situ* hybridization with 11$\beta$-HSD2 cDNA on normal human adult kidney (Figure 6) showed abundant 11$\beta$-HSD2 mRNA expression restricted to the distal nephron (distal convoluted tubule, cortical collecting duct and medullary collecting ducts), with no specific hybridization in other regions (glomerulus, proximal tubule, etc.). Expression in the distal convoluted tubule extended to loops participating in juxtaglomerular complexes. There was no hybridization in sense controls. There was also abundant expression of 11$\beta$-HSD2 mRNA in human placental trophoblast (results not shown).

The nature of the $\sim$ 4 kb 11$\beta$-HSD2-hybridizing transcript in fetal kidney is unclear. Interestingly, flanking duplications involving the genes encoding human steroid-metabolizing enzymes are common (e.g. 17$\beta$-HSD type 1, the 3$\beta$-HSD family, 5$\alpha$-reductase type 1, 21-hydroxylase and 17$\beta$-HSD type 4), and duplicates are often transcribed, either as separate transcripts or, in the case of 17$\beta$-HSD4, as a large transcript traversing the apparent gene duplication.

### Immunohistochemistry

Antisera raised to a synthetic 11$\beta$-HSD2 peptide (residues 370–383) coupled to keyhole limpet haemocyanin identified a single strong protein band at $\sim$ 40000-$M_r$ in Western blots of human placenta and kidney tissue extracts (Figure 7a). This was also detected in CHO cells transfected with 11$\beta$-HSD2 cDNA, but not in untransfected controls. This band was not observed when the antisera were preabsorbed with 11$\beta$-HSD2-(370–383)-peptide. An additional, much weaker, band was seen at $\sim$ 70000-$M_r$ in some kidney extracts. Immunohistochemistry on human placenta revealed dense immunostaining of the trophoblast (in the syncytiotrophoblast layer), but not the decidua (Figure 7b). Very dense immunostaining in adult human kidney (Figure 7c) was seen localized to the distal nephron (distal convoluted tubule including juxtaglomerular loops, cortical and medullary collecting ducts). In both tissues the immunostaining was abolished by preabsorption with 11$\beta$-HSD2-(370–383)-peptide (Figures 7b and 7c). Neither tissue showed any immunostaining using preimmune serum (results not shown).

*In situ* hybridization and immunohistochemistry demonstrated abundant 11$\beta$-HSD2 mRNA and protein in kidney in the location expected (distal nephron) for 11$\beta$-HSD2 to confer aldosterone selectivity on mineralocorticoid receptors. 11$\beta$-HSD2 expression in the distal convoluted tubule extends into loops participating in juxtaglomerular complexes. In placenta 11$\beta$-HSD2 expression was abundant in the syncytiotrophoblast lining the placental villi, thus being at the very interface between the fetal tissue and maternal blood, which flows in the intervillus spaces. This is exactly the location which would allow 11$\beta$-HSD2 the greatest influence over the passage of maternal glucocorticoid to the fetus.

### Developmental expression

Two studies, using tissue slices from fetuses at 10–20 weeks gestation [49] or adding $NAD^+$ to tissue homogenates from 16–19-week fetuses [12], have found substantial levels of 11$\beta$-dehydrogenase activity in almost all human fetal tissues (including kidney, lung and brain). Fetal liver was found to have net 11$\beta$-reductase in the first study and an $NAD^+$-dependent 11$\beta$-dehydrogenase in the second. We found no 11$\beta$-HSD2 hybridization in fetal lung, liver or brain. As 11$\beta$-HSD1 mRNA is reported absent at least from fetal lung and liver [12], it is possible that a third 11$\beta$-HSD isoform is expressed in the fetus. However, as our samples were from fetuses slightly later in gestation it is possible that 11$\beta$-HSD2 expression, while present

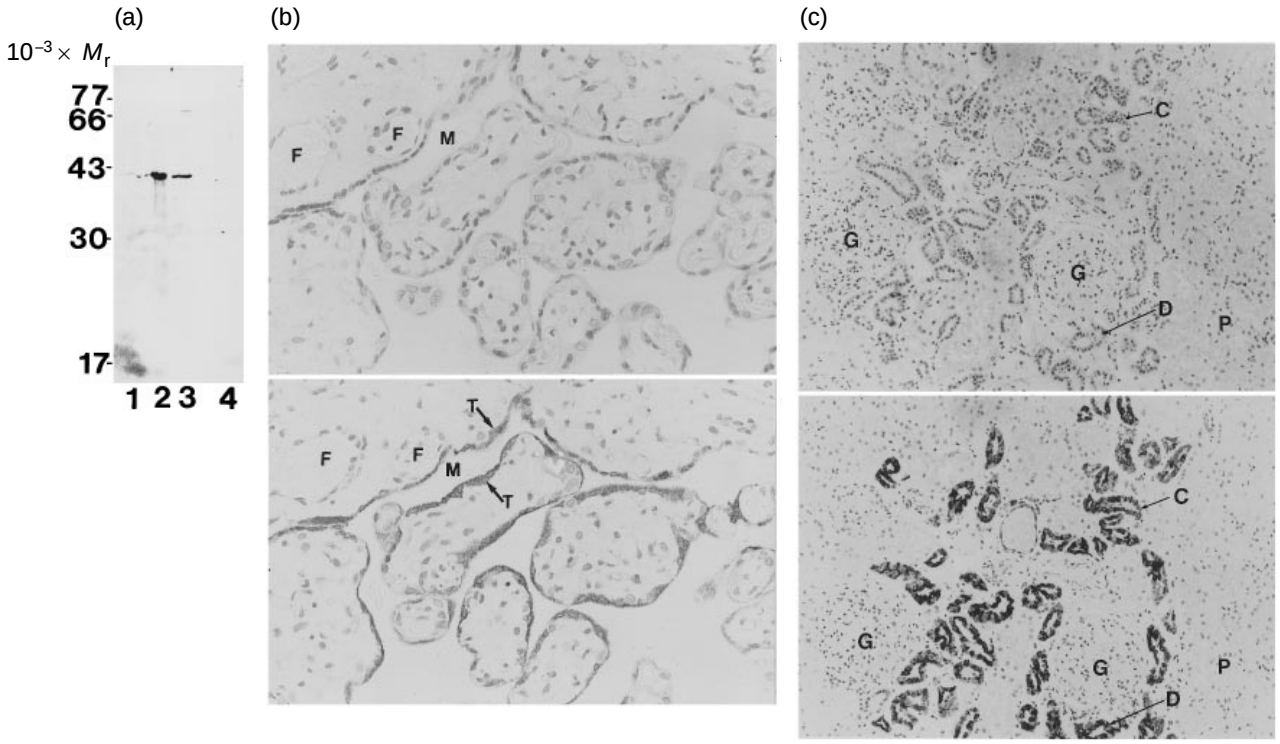


**Figure 7 Studies with antisera to human placental 11$\beta$-HSD2-(370–383)-peptide**

(**a**) Western blot using anti-11$\beta$-HSD2 antisera and blotted tissue subfractions (25000 $g$ pellet; mainly heavy microsomes and mitochondria) from: CHO cells transfected with (lane 1) and without (lane 4) 11$\beta$-HSD2 cDNA, human placenta (lane 2) and human adult kidney (lane 3). Positions of protein standards are indicated. (**b**) and (**c**) Immunohistochemistry on (**b**) human placenta and (**c**) human adult kidney with haematoxylin counterstaining (stains nuclei). Lower panels, antisera to human placental 11$\beta$-HSD2-(370–383)-peptide; upper panels, control with antisera preabsorbed with the 11$\beta$-HSD2-(370–383)-peptide. Panel (**b**) shows a high-power view of placental villi cut cross-sectionally. Fetal blood circulates in fetal capillaries (two are marked F) within the villi, maternal blood occupies the intervillus space (marked M), and abundant 11$\beta$-HSD2 expression is localized in the syncytiotrophoblast layer (T) which intervenes between the fetal and maternal circulations. Panel (**c**) shows a medium-power view of human kidney cortex. The following are labelled: G, glomerulus; D, distal convoluted tubule; P, area with proximal tubules; C, cortical collecting duct. Clearly the 11$\beta$-HSD2 protein is abundant in the distal nephron.

during early gestation, is switched off in many fetal tissues (the kidney being a clear exception) at mid-gestation (specifically before 22–23 weeks in lung, 22–26 weeks in liver and 21–26 weeks in brain). Indeed, our preliminary studies on mouse development support this pattern of expression (R. W. Brown, R. Diaz and J. R. Seckl, unpublished work). The mechanism of such developmental control is unknown but, interestingly, it seems that a CpG island may be associated with 5′ regulatory regions of the 11$\beta$-HSD2 gene, since: (1) the CpG island extends to the very start of the 11$\beta$-HSD2 clone, (2) from the 11$\beta$-HSD2 transcript size on Northern blots it appears that the p11$\beta$2 clone must be approximately full length (although we have not precisely mapped the start site) and (3) CpG islands are large (typically $> 1$ kb) and often include the most 5′ exon as well as upstream sequences [30]. This is intriguing because CpG islands are often methylated in tissues where the gene is not expressed. Silencing of the expression of genes with 5′ CpG islands may be associated with methylation of the CpG island. Whether a regulatory influence of this kind occurs in the 11$\beta$-HSD2 gene remains to be elucidated. Work on baboon pregnancy suggests that the 11$\beta$-HSD barrier to maternal glucocorticoids only becomes firmly established after mid-gestation [48,50]; prior to this fetal tissues may express 11$\beta$-HSD2 and 'protect themselves' from high maternal glucocorticoid levels. As the placenta takes over the protective role, fetal tissues adopt a much more 'adult' 11$\beta$-HSD2 expression pattern and fetal adrenal activity may begin to dictate their glucocorticoid exposure.

## Conclusion

The human placental cDNA that we have isolated encodes an enzyme with the expected characteristics of 11$\beta$-HSD2 activity in placenta. The location of 11$\beta$-HSD2 mRNA and protein in human tissues supports its proposed key roles as a modulator of glucocorticoid action and mineralocorticoid receptor specificity and as a major determinant of the glucocorticoid exposure of the developing fetus.

It is unlikely that a direct X-ray-crystallography-derived structure will be available in the near future for 11$\beta$-HSD2 (which is an intrinsic membrane protein). We have presented its predicted secondary structure in some detail. This will be of particular relevance, as mutations are sought in the protein which may explain: (i) the dramatic loss of 11$\beta$-HSD2 enzyme activity that appears to occur in the syndrome of apparent mineralocorticoid excess (SAME), (ii) the more subtle variations in 11$\beta$-HSD activity indicated by the altered urinary glucocorticoid metabolites described in subsets of patients with essential hypertension [51] or polycystic ovary disease [52], or (iii) the impaired placental 11$\beta$-HSD2 activity which correlates with reduced birth weight in humans [6].

Finally, two further points remain unexplained. First, why does 11$\beta$-HSD2, which metabolizes a hydrophobic substrate using a positively charged cofactor ($NAD^+$), possess such a positively charged structure? Secondly, if mutations in 11$\beta$-HSD2 cause SAME, how do the associated alterations in 5$\alpha$/5$\beta$-reductase activity [53,54] come about, as 11$\beta$-HSD2 appears to have neither activity? Clearly further studies of this key enzyme, 11$\beta$-HSD2, will not only shed light on such matters but are likely to contribute to a better understanding of the role of corticosteroid physiology in development and the aetiology of hypertension in humans.

### Note added in proof. (received 13 November 1995)

After completion of this work the first crystal structure for 17$\beta$-HSD1 has been reported [55], showing an N-terminal SCAD region followed by $\alpha$-helices and a flexible C-terminal region. This is intriguingly similar to the structure predicted above for 11$\beta$-HSD2.

This work was supported by an MRC Training Fellowship (R.W.B.) (grant no. G84/2857), and grants from The Wellcome Trust (J.R.S.) and The Scottish Hospital Endowments Research Trust. We thank Dr. Bala Ramesh for synthesizing 11$\beta$-HSD2-(370–383)-peptide and Dr. Brian McGinn for coupling it to carrier protein for immunization.

## REFERENCES

1 Seckl, J. R. and Brown, R. W. (1994) J. Hypertens. **12**, 105–112
2 Edwards, C. R. W., Benediktsson, R., Lindsay, R. S. and Seckl, J. R. (1993) Lancet **341**, 355–357
3 Murphy, B. E., Clark, S. J., Donald, I. R., Pinsky, M. and Vedady, D. (1974) Am. J. Obstet. Gynecol. **118**, 538–541
4 Beitins, I. Z., Bayard, F., Ances, I. G., Kowarski, A. and Migeon, C. J. (1973) Pediatr. Res. **7**, 509–519
5 Benediktsson, R., Lindsay, R. S., Noble, J., Seckl, J. R. and Edwards, C. R. W. (1993) Lancet **341**, 339–341
6 Benediktsson, R., Noble, J., Calder, A. A., Edwards, C. R. W. and Seckl, J. R. (1995) J. Endocrinol. **144** (Suppl.), 160
7 Barker, D. J. P. (1991) Fetal Origins of Adult Disease, BMJ Publications, London
8 Lakshmi, V. and Monder, C. (1988) Endocrinology (Baltimore) **123**, 2390–2398
9 Brown, R. W., Chapman, K. E., Edwards, C. R. W. and Seckl, J. R. (1993) Endocrinology (Baltimore) **132**, 2614–2621
10 Naray-Fejes-Toth, A., Rusvai, E., Denault, D. L., St Germain, D. L. and Fejes-Toth, G. (1993) Am. J. Physiol. **265**, F896–F900
11 Yang, K. and Yu, M. (1994) J. Steroid Biochem. Mol. Biol. **49**, 245–250
12 Stewart, P. M., Murry, B. A. and Mason, J. I. (1994) J. Clin. Endocrinol. Metab. **78**, 1529–1532
13 Funder, J. W., Pearce, P. T., Smith, R. and Smith, A. I. (1988) Science **242**, 583–585
14 Edwards, C. R. W., Stewart, P. M., Burt, D., Brett, L., McIntyre, M. A., Sutanto, W. S., de Kloet, E. R. and Monder, C. (1988) Lancet **2**, 986–989
15 Brown, R. W., Chapman, K. E., Murad, P., Edwards, C. R. W. and Seckl, J. R. (1996) Biochem. J. **313**, 997–1005
16 Chomczynski, P. and Sacchi, N. (1987) Anal. Biochem. **162**, 156–159
17 Israel, D. L. (1993) Nucleic Acids Res. **21**, 2627–2631
18 Murphy, A. J. M., Kung, A. L., Swirski, R. A. and Schimke, R. T. (1992) Methods Companion Methods Enzymol. **4**, 111–131
19 Rysavy, F. R., Bishop, M. J., Gibbs, G. P. and Williams, G. W. (1995) Comput. Appl. Biosci. **8**, 149–154
20 Rost, B. and Sander, C. (1994) Proteins **19**, 55–72
21 Genetics Computer Group (1994) Program Manual for the Wisconsin Package, 8th edn., Science Drive, Madison, WI
22 Chou, P. Y. and Fasman, G. D. (1978) Adv. Enzymol. **47**, 45–148
23 Nishikawa, K. (1983) Biochim. Biophys. Acta **748**, 285–299
24 Garnier, J., Osguthorpe, D. J. and Robson, B. (1978) J. Mol. Biol. **120**, 97–103
25 Kyte, J. and Doolittle, R. F. (1982) J. Mol. Biol. **157**, 105–132
26 Karplus, P. A. and Schulz, G. E. (1985) Naturwissenschaften **72**, 212–213
27 Emini, E. A., Hughes, J. V., Perlow, D. S. and Boger, J. (1985) J. Virol. **55**, 836–839
28 Low, S. C., Chapman, K. E., Edwards, C. R. W. and Seckl, J. R. (1994) J. Mol. Endocrinol. **13**, 167–174
29 Yau, J. L. W., Kelly, P. A. T., Sharkey, J. and Seckl, J. R. (1994) Neuroscience **61**, 31–40
30 Bird, A. P. (1986) Nature (London) **321**, 209–213
31 Kozak, M. (1987) Nucleic Acids Res. **15**, 8125–8128
32 Persson, B., Krook, M. and Jornvall, H. (1991) Eur. J. Biochem. **200**, 537–543
33 Ghosh, D., Weeks, C. M., Grochulski, P., Duax, W. L., Erman, M., Rimsay, R. L. and Orr, J. C. (1991) Proc. Natl. Acad. Sci. U.S.A. **88**, 10064–10068
34 Marchesi, V. T., Furthmayr, H. and Tomita, M. (1976) Annu. Rev. Biochem. **45**, 667–695
35 Wu, L., Einstein, M., Geissler, W. M., Chan, H. K., Elliston, K. O. and Andersson, S. (1993) J. Biol. Chem. **268**, 12964–12969
36 Marks, A. R., McIntyre, J. O., Duncan, T. M., ErdjumentBromage, H., Tempst, P. and Fleischer, S. (1992) J. Biol. Chem. **267**, 15459–15463
37 Tannin, G. M., Agarwal, A. K., Monder, C., New, M. I. and White, P. C. (1991) J. Biol. Chem. **266**, 16653–16658
38 Agarwal, A. K., Mune, T., Monder, C. and White, P. C. (1994) J. Biol. Chem. **269**, 25959–25962
39 Albiston, A. L., Obeyesekere, V. R., Smith, R. E. and Krozowski, Z. S. (1994) Mol. Cell. Endocrinol. **105**, R11–R17
40 Cheng, K.-C., White, P. C. and Qin, K.-N. (1991) Mol. Endocrinol. **5**, 823–828
41 Pawlowski, J. E., Huizinga, M. and Penning, T. M. (1991) J. Biol. Chem. **266**, 8820–8825
42 Naville, D., Keeney, D. S., Jenkin, G., Murray, B. A., Head, J. R. and Mason, J. I. (1991) Mol. Endocrinol. **5**, 1090–1100
43 Zhao, H. F., Labrie, C., Simard, J., De Launoit, Y., Trudel, C., Martel, C., Rheaume, E., Dupont, E., Luu-The, V., Pelletier, G. and Labrie, F. (1991) J. Biol. Chem. **266**, 583–593
44 Paabo, S., Bhat, B. M., Wold, W. S. M. and Peterson, P. A. (1987) Cell **50**, 311–317
45 Shin, J., Dunbrack, R.L, Jr., Lee, S. and Strominger, J. L. (1991) Proc. Natl. Acad. Sci. U.S.A. **88**, 1918–1922
46 Feldman, D., Funder, J. W. and Edelman, I. S. (1973) Endocrinology (Baltimore) **92**, 1429–1441
47 Naray-Fejes-Toth, A., Rusvai, E. and Fejes-Toth, G. (1994) Endocrinology (Baltimore) **134**, 1671–1675
48 Albrecht, E. D. and Pepe, G. J. (1990) Endocr. Rev. **11**, 124–150
49 Murphy, B. E. (1981) J. Steroid Biochem. **14**, 811–817
50 Pepe, G. J., Waddell, B. J., Stahl, S. J. and Albrecht, E. D. (1988) Endocrinology (Baltimore) **122**, 78–83
51 Soro, A., Ingram, M. C., Tonolo, G., Glorioso, N. and Fraser, R. (1995) Hypertension **25**, 67–70
52 Rodin, A., Thakkar, H., Taylor, N. and Clayton, R. (1994) N. Engl. J. Med. **330**, 460–465
53 Ulick, S., Levine, L. S., Gunczler, P., Arriza, J. L., Weinberger, C., Cerelli, G., Glaser, T. M., Handelin, B. L., Houseman, D. E. and Evans, R. M. (1979) J. Clin. Endocrinol. Metab. **49**, 757–764
54 Monder, C., Shackleton, C. H., Bradlow, H. L., New, M. I., Stoner, E., Iohan, F. and Lakshmi, V. (1986) J. Clin. Endocrinol. Metab. **63**, 550–557
55 Ghosh, D., Pletnev, V. Z., Zhu, D.-W., Wawrzak, Z., Daux, W. L., Pangborn, W., Labrie, F. and Lin, S.-X. (1995) Structure **3**, 503–513

Received 26 June 1995/11 September 1995; accepted 27 September 1995